ENVIRONMENTAL RESEARCH
LETTERS

LETTER • OPEN ACCESS

The evolution of the Fram Strait sea ice volume export decomposed by age: estimating with parameter-optimized sea ice-ocean model outputs

To cite this article: Yijun Yang *et al* 2023 *Environ. Res. Lett.* **18** 014029

ENVIRONMENTAL RESEARCH
LETTERS

CrossMark

OPEN ACCESS

RECEIVED
13 April 2022

REVISED
22 December 2022

ACCEPTED FOR PUBLICATION
30 December 2022

PUBLISHED
11 January 2023

LETTER

The evolution of the Fram Strait sea ice volume export decomposed by age: estimating with parameter-optimized sea ice-ocean model outputs

Yijun Yang[1], Chao Min[1,2], Hao Luo[1,*], Frank Kauker[2], Robert Ricker[3] and Qinghua Yang[1]

[1] School of Atmospheric Sciences, Sun Yat-sen University, and Southern Marine Science and Engineering Guangdong Laboratory (Zhuhai), 519082 Zhuhai, People's Republic of China
[2] Alfred Wegener Institute, Helmholtz Centre for Polar and Marine Research, 27570 Bremerhaven, Germany
[3] NORCE Norwegian Research Centre, Tromsø 9019, Norway
[*] Author to whom any correspondence should be addressed.

E-mail: luohao25@mail.sysu.edu.cn

Keywords: sea ice volume flux, Fram Strait, sea ice age, Arctic

Abstract

Sea ice export through the Fram Strait is crucial in the dynamic evolution of Arctic sea ice and can further modulate Arctic sea ice mass balance as well as the ocean thermohaline circulation. In this study, based on outputs from a parameter-optimized and fully physical ocean–sea ice coupled model and sea ice age observation, we estimate sea ice volume (SIV) flux and its age evolution via the Fram Strait. The estimate of mean annual SIV flux is about 1605 ± 315 km^3 yr^{-1} without a significant trend for 1979–2021. Combining with sea ice age data, the variation of the sea ice age and its corresponding SIV flux are obtained for 1984–2020. The SIV flux of 1st-year ice significantly increases as expected, but it still contributes very little to the total flux in the 2010s with a proportion of 3.5%. SIV fluxes of different ages in multi-year ice present diverse variations. The proportions of 2nd-year ice and 3rd-year ice in the annual SIV flux show an extreme increase from 6.8% and 25.0% in the 1980s to 49.0% and 38.8% in the 2010s, respectively, while the proportions of 4th-year ice and 5th-year and older (5+ year) ice significantly decrease from 22.8% and 45.0% in the 1980s to 7.1% and 1.6% in the 2010s, respectively. Meanwhile, the prevailing age of annual volume export via Fram Strait shifts from 4th-year and 5+ year ice to 2nd-year and 3rd-year ice around 2007/2008. It is worth noticing that the variation in Fram Strait ice export modulates the variation in Arctic SIV prior to 2008, but the reverse is true after 2008, indicating a decreasing influence of Fram Strait SIV export on Artic SIV variability with decreasing sea ice age. The results are beneficial to promote the understanding of the evolution of Fram Strait SIV export under the warming Arctic.

1. Introduction

With the accelerated Arctic warming, the Arctic sea ice dramatically retreated during the last decades. In particular, the Arctic sea ice extent (SIE) in September retreated 12.8 ± 2.3% per decade from 1979 to 2018 (Meredith *et al* 2019). Bi *et al* (2018a) reported that compared with the period from 2003 to 2008, the autumn Arctic sea ice volume (SIV) decreased in the period from 2011 to 2015 and about 87% of this change could be attributed to the depletion of multi-year ice (MYI). Thus, thinner and younger sea ice is increasingly present in the Arctic (Maslanik *et al* 2007, Kwok and Rothrock 2009, Kwok 2018). These changes are reflected in spatial SIV anomalies that are the results of the interaction between dynamics and thermodynamics (Ricker *et al* 2021). Quantifying SIV fluxes is crucial to estimate the impact of sea ice dynamics on sea ice mass balance changes in the Arctic.

The Fram Strait, located between Greenland and the Svalbard Archipelago (figure 1(a)), is a major outlet for Arctic sea ice and an important passage connecting the Arctic and the Atlantic. Sea ice export through the Fram Strait accounts for 90% of the

Arctic sea ice outflow and the annual export is about 13% of total Arctic sea ice mass on average (1980–2000) (Serreze *et al* 2006, Haine *et al* 2015). Considering the dramatical changes in the oldest ice type of the Arctic sea ice during the past few decades (Maslanik *et al* 2011, Kwok 2018), sea ice export through the Fram Strait may have potential influences on the variability of the Arctic MYI (Ricker *et al* 2018).

Previously, observations and model datasets have all been used to estimate the Fram Strait SIV flux. For instance, based on sea ice thickness (SIT) from upward looking sonars (ULS), Spreen *et al* (2020) calculated the long-term variability of SIV export from 1992 to 2014. With the availability of SIT retrievals from ICESat and CryoSat-2, several studies provided SIV flux estimations in freezing seasons (e.g. Spreen *et al* 2009, Bi *et al* 2018b, Ricker *et al* 2018). Nevertheless, gaps remain because of the spatial scarcity of the *in-situ* observations and the challenges of retrieving SIT from satellites during melting seasons. Recently long-term estimates based on non-assimilated model outputs (e.g. Wei *et al* 2019, Zamani *et al* 2019) showed overestimation compared with satellite-derived results due to overestimations of simulated SIT and sea ice drift (SID) on the gate. The Fram Strait SIV flux was also estimated by applying reanalyzes of SIT (e.g. Zhang *et al* 2017, Min *et al* 2019). It is also worth noting that these reanalyzes only adjust the specified model variables during assimilation, which is not dynamically consistent (Balmaseda *et al* 2015). Furthermore, given the ability to preserve the model's conservation compared to reanalyzes and the fact that they are closer to observations than the output from the model free run, outputs of parameters-optimized models are also valuable data sources for studies of the Arctic sea ice. For instance, Ricker *et al* (2021) pointed out that the North Atlantic/Arctic Ocean Sea Ice Model (NAOSIM) optimized by the micro-genetic algorithm outperforms the Pan-Arctic Ice Ocean Modeling and Assimilation System (PIOMAS) in reproducing the stabilizing mechanism for negative ice growth feedback in the marginal seas bordering North America and Asia. The Fram Strait SIV export should therefore be reevaluated in light of NAOSIM data.

In addition, the changes in the Arctic sea ice age featuring first-year ice (FYI) advance and MYI depletion during the past few decades (Maslanik *et al* 2011, Bi *et al* 2018a) also have influences on sea ice outflow through the Fram Strait. However, whether the FYI has already become the main part of sea ice outflow is unclear. Moreover, sea ice over the Fram Strait is typically divided into FYI and MYI in previous studies, and conclusions about MYI are mainly drawn regarding MYI as a whole. For example, Wang *et al* (2022) indicated a large decline in the proportion of MYI in the area exported via the Fram Strait, which decreased from 72% in 2002/2003–2010/2011 to 59% in 2012/2013–2019/2020. Ricker *et al* (2018) illustrated that the variation of MYI volume export through the Fram Strait contributes 54% of the Arctic MYI volume variability in freezing seasons. While, MYI is still not further classified in accordance with the sea ice age. However, as MYI is made up of different ice ages that exhibit different characteristics (Bi *et al* 2016, Tschudi *et al* 2016), it is necessary to examine whether the evolution of MYI at various ice ages is compatible with the evolution of MYI as a whole and whether the relation between SIV export and Arctic SIV has changed when the age composites in SIV outflow change. Therefore, it is crucial to fill the gap in the distinguishment of SIV export through the Fram Strait by sea ice age groups combined with a continuous sea ice age dataset.

2. Data and methods

2.1. NAOSIM sea ice data

NAOSIM is a regional sea ice-ocean model developed by the Alfred Wegener Institute (Gerdes *et al* 2003, Kauker *et al* 2005, Karcher *et al* 2007, 2011). The model grid covers the whole Arctic and the northern North Atlantic Ocean (north of approximately 50° N) by a spherical rotated grid. The model is driven by atmospheric forcing's from the NCEP Climate Forecast System Reanalysis Climate Forecast System version 2 (NCEP-CFSR-CFSv2, Saha *et al* 2014). Sumata *et al* (2019a, 2019b) developed the sea ice model by optimizing fifteen sea ice and ocean model parameters simultaneously using a micro genetic algorithm (mGA). Compared to the adjoint approach which linearizes the physical model and results in exponentially growing perturbations, the mGA approach applies the full nonlinear original physical model system, which is more physically reasonable (Sumata *et al* 2019a). In addition, the usefulness of mGA and the robustness of the simulated sea ice climatology, trend, and interannual variability were verified by testing 11 optimization experiments (Sumata *et al* 2019a). The modeled sea ice data used in this study is the medium-resolution version (28 km × 28 km) of NAOSIM daily effective SIT and SID data from January 1979 to October 2021. The simulated SIT and SID we used are from the third optimization version (Sumata *et al* 2019a). For more details can refer to Sumata *et al* (2019a, 2019b).

2.2. NSIDC sea ice age data

The 'EASE-Grid Sea Ice Age (Version 4)' product (Tschudi *et al* 2019b) provides weekly sea ice age from 1984 to 2020 with a spatial resolution of 12.5 km. The ice parcels are marked as FYI firstly in 1978 and then tracked as Lagrangian parcels following the weekly

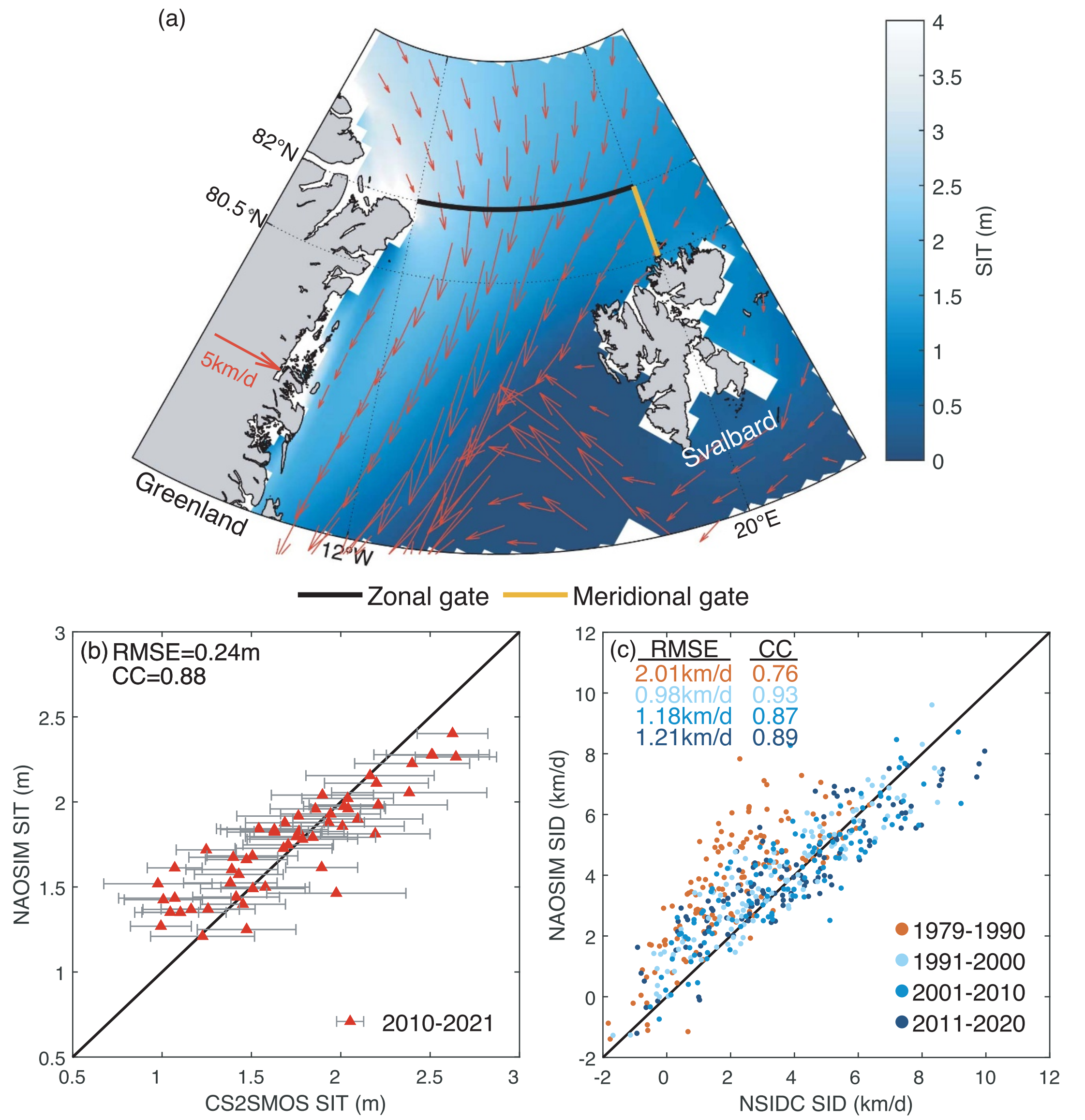

Figure 1. (a) The spatial pattern of multi-decadal (1979–2020) annual mean NAOSIM SIT (shading) and SID (arrows). The black and yellow lines show the zonal gate and meridional gate of the Fram Strait defined in this study, respectively. The zonal gate locates between 12° W and 20° E along 82° N, and the meridional gate locates between 80.5° N and 82° N along 20° E. (b) Scatter plot of monthly SIT (averaged on the Fram Strait) of NAOSIM and CS2SMOS from November to March from 2010 to 2021. (c) Scatter plot of monthly SID (averaged on the Fram Strait) of NAOSIM and NSIDC for four periods (1979–1990, 1991–2000, 2001–2010, and 2011–2020). Note that solid black lines in figures (b) and (c) are 1–1 lines, the error bar in figure (b) represents the uncertainty of CS2SMOS.

'Polar Pathfinder Daily 25 km EASE-Grid Sea Ice Motion Vectors (version 4.1)' (Tschudi *et al* 2019a). All parcels age one year during the week of Arctic sea ice minimum extent and will no longer be considered up to 16 yr or the SIC of a grid cell is less than 15%. The age of a certain grid cell is always assigned as the oldest parcel within the grid, therefore this product could effectively estimate the oldest ice parcels. Tschudi *et al* (2020) evaluated the version 4 age product compared with the preceding version and indicated its improvement in the continuity of the age field and performance in MYI. More details can be found in Tschudi *et al* (2020).

2.3. Methods

Following Krumpen *et al* (2016) and Ricker *et al* (2018), we define the Fram Strait as a composite gate that consists of zonal and meridional gates, which have been chosen for lower errors and bias in satellite SIT and SID data. The zonal gate is defined as the passage between 12° W and 20° E along 82° N, while the meridional gate is defined as the passage between 80.5° N and 82° N along 20° E (figure 1(a)). For the calculation of SIV fluxes, daily NAOSIM SIT and SID data are interpolated onto the zonal and meridional gates firstly with the grid spatial resolutions of 1° and 0.15°, respectively, which is to get similar grid lengths on the zonal and meridional gates. Then SIV fluxes could be derived by following Ricker *et al* (2018) and Min *et al* (2019):

$$Q_x = L_x H_x v \tag{1}$$

$$Q_y = L_y H_y u \tag{2}$$

where Q is SIV flux, L represents length of the grids, H represents the modeled effective SIT, and the subscript x and y correspond to variables on the zonal gate and meridional gate, respectively. Moreover, v and u represent sea ice velocities perpendicular to the zonal gate and meridional gate, respectively. SIV flux of each gate is obtained by summing up fluxes of all grids on that gate, then the total volume flux through the Fram Strait is the aggregate of the fluxes on the zonal and meridional gates. The southward (westward) flux through the zonal (meridional) gate is defined as positive flux (Selyuzhenok *et al* 2020).

We further calculate the volume flux differentiated by sea ice ages. The weekly sea ice age data are averaged to monthly data and interpolated onto the Fram strait as methods introduced above. Then we sum the monthly fluxes of grids that have the same age to calculate the annual total flux of different sea ice ages. In this study, the annual period is considered from October to September following previous studies (e.g. Kwok *et al* 2004, Wei *et al* 2019), and the cold (warm) season is specified from October (May) to April (September) (Spreen *et al* 2009, Ricker *et al* 2018). Generally, the investigation period for SIV flux is from October 1979 to September 2021 according to the availability of NAOSIM and the annual time window. The study period is from October 1984 to September 2020 when combining SIV flux with the sea ice age data. Throughout the study, trends and correlation coefficients are statistically significant when the confidence level of the Student t-test exceeds 95%.

3. Results

3.1. Model validation

To validate the performance of NAOSIM sea ice data at the Fram Strait, we show scatter plots between monthly NAOSIM and satellite SIT also SID at the Fram Strait in figures 1(b) and (c), respectively. The satellite SIT data is the weekly CS2SMOS (v204) data generated at the Alfred Wegener Institute Helmholtz Center for Polar and Marine Research (AWI), which merges CryoSat-2 (CS2) and Soil Moisture and Ocean Salinity (SMOS) satellite data (Ricker *et al* 2017). The CS2SMOS product is a good reference for SIT validation in the Fram Strait, where mixed ice types can often be found. In figure 1(b), generally, scatters distribute closely to the 1–1 line and the 1–1 line is typically within the uncertainty of CS2SMOS SIT. Thus, NAOSIM SIT is comparable with CS2SMOS in cold seasons from 2010 to 2021. NAOSIM performs well at the correlation ($CC = 0.88$) and root-mean-square error ($RMSE = 0.24$ m) compared with CS2SMOS, although NAOSIM shows a little overestimation of thin ice and underestimation of thick ice. NAOSIM SID from 1979 to 2020 is compared with the daily 'Polar Pathfinder Daily 25 km EASE-Grid Sea Ice Motion Vectors (version 4.1)' (Tschudi *et al* 2019a) distributed by the National Snow and Ice Data Center (NSIDC). The significantly high CC values between NAOSIM and NSIDC SID for four periods show reliable variability of NAOSIM SID on the gate (figure 1(c)). Before the 1990s, the scatters are mostly above a 1–1 line, indicating that NAOSIM SID is a little faster than NSIDC SID. However, NSIDC SID is slower and less variable in the 1980s owing to the lack of buoys (Zamani *et al* 2019, Tschudi *et al* 2020). Since the 1990s (i.e. 1991–2000, 2001–2010, and 2011–2020), scatters are mainly surrounding the 1–1 line, therefore NAOSIM SID is more consistent with NSIDC SID. The RMSE values also become smaller in 1991–2000, 2001–2010, and 2011–2020 compared to 1979–1990. In summary, NAOSIM data can well reproduce the Fram Strait sea ice parameters and provide reliable sea ice estimations for quantifying SIV fluxes through the Fram Strait.

3.2. SIV export through the Fram Strait

Combining NAOSIM SIT and SID, we estimate the variabilities of annual, cold-season, and warm-season SIV fluxes through the Fram Strait (figure 2(a)). The mean annual SIV flux from 1979/1980–2020/2021 is about 1605 ± 315 km^3 yr^{-1}. On average, 71 ± 4% of the interannual variability of annual flux comes from the cold-season flux (1146 ± 240 km^3 yr^{-1}), which is nearly 2.5 times of the warm-season flux (459 ± 108 km^3 yr^{-1}). The annual SIV flux peaks in 1994/1995 (2321 km^3 yr^{-1}) while the minimum SIV fluxes occur in 2017/2018 (999 km^3 yr^{-1}). The peak value in 1994/1995 was also reported by previous studies (e.g. Kwok *et al* 2004, Zhang *et al* 2017, Wei *et al* 2019), which may have been caused by a significant anomalous southward SID at the Fram Strait (Arfeuille *et al* 2000). While the minimum value in 2017/2018 can be attributed to regional sea ice-ocean processes driven by abnormally atmospheric circulation over the Atlantic Arctic Ocean (Sumata *et al* 2022). Meanwhile, linear regressions indicate that none of the annual, cold-season, and warm-season SIV fluxes has an obvious trend from 1979 to 2021.

Figure 2(b) shows the annual cycle of monthly SIV flux, SID, and SIT through the Fram Strait. Annually, more than 84% of SIV flux is from the zonal gate, even occupying more than 97% from July to September. The annual cycle of SIV flux (zonal gate plus meridional gate) amounts between 198.5 km^3 month^{-1} (March) and 42.1 km^3 month^{-1} (August). The annual cycle of SID is the fastest (5.11 km d^{-1}) in

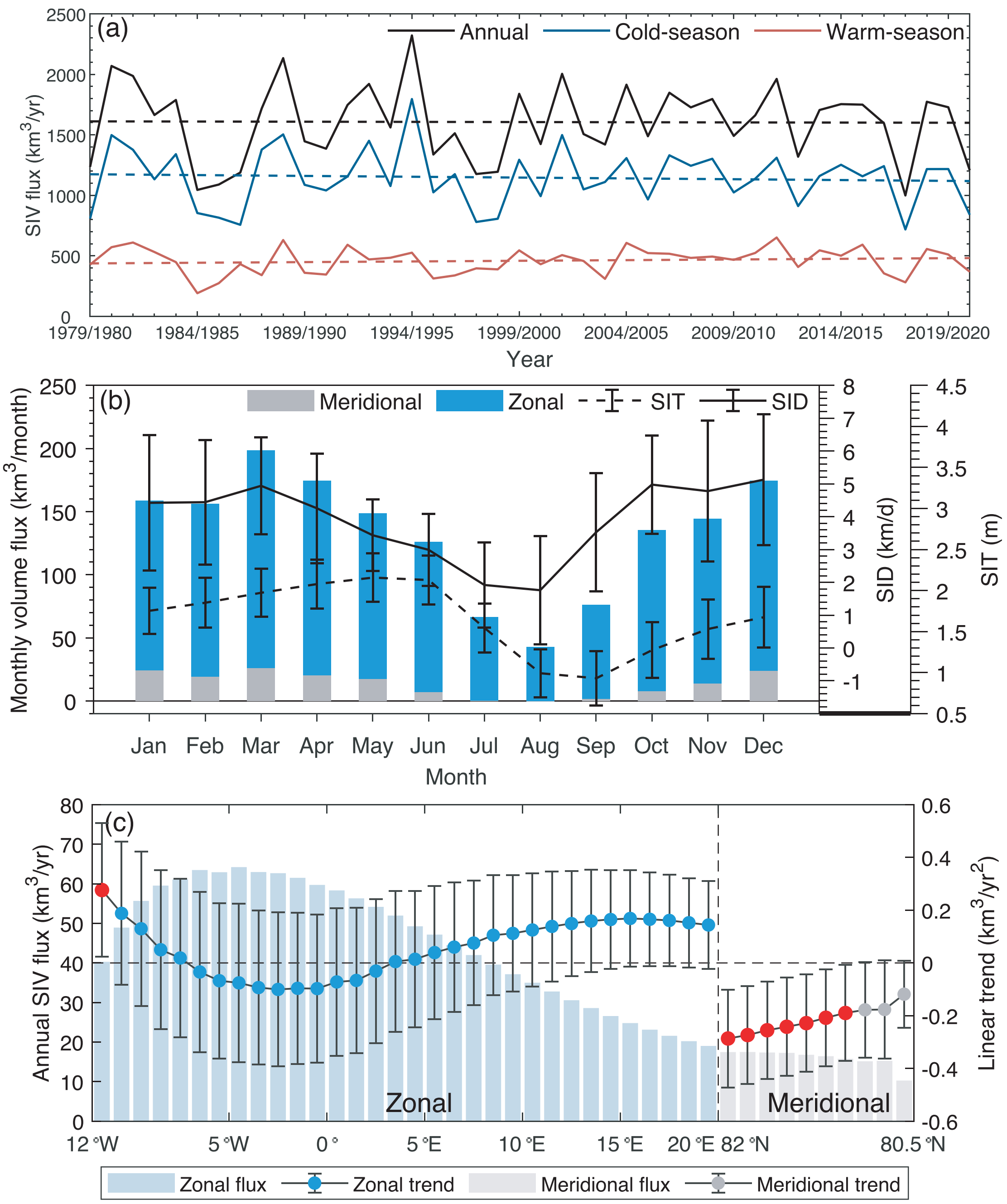

Figure 2. (a) Time series (solid line) and linear regressions (dashed line) of annual (black line), cold-season (blue line), and warm-season (red line) volume flux through the Fram Strait from 1979/1980–2020/2021. (b) Multi-decadal averaged (1979–2020) annual cycle of monthly SIV flux through the zonal gate (blue shading bar) and the meridional gate (gray shading bar) of the Fram Strait, and annual cycle of monthly SID (solid black line) and SIT (dashed black line) at the Fram Strait. (c) The left axis corresponds to the long-term mean (average from 1979/1980–2020/2021) annual SIV flux of the zonal gate (blue bar) and the meridional gate (gray bar). The right axis shows linear trend (1979/1980–2020/2021) of the annual SIV flux of each grid on the zonal gate (line with blue points) and the meridional gate (line with gray points) with the 95% confidence intervals as the error bar. Statistically significant trends at a 95% confidence level are shown in red points. The horizontal dashed line refers to the zero line for the linear trend, and the vertical dashed line partitions the result of the zonal gate and the meridional gate.

March and the slowest (1.81 km d^{-1}) in August, which is in phase with the annual cycle of volume flux. While SIT is the thickest in May (2.16 m), and the thinnest in September (0.93 m) and lags behind SIV. The coefficient of determinations (R^2) between the standardized monthly SIV flux and SIT/SID from 1979 to 2021 is calculated to figure out the determinative factor that influences SIV flux variability (Ricker *et al* 2018, Min *et al* 2019). The result shows that SID is the main factor that regulates the variation of monthly SIV flux with R^2 of 0.74, which is more than twice the R^2 between SIT and SIV flux (0.30).

The spatial distribution of the long-term trend and the long-term mean of the annual SIV flux on the Fram Strait is shown in figure 2(c). Spatial differences can be found both in the tendency and

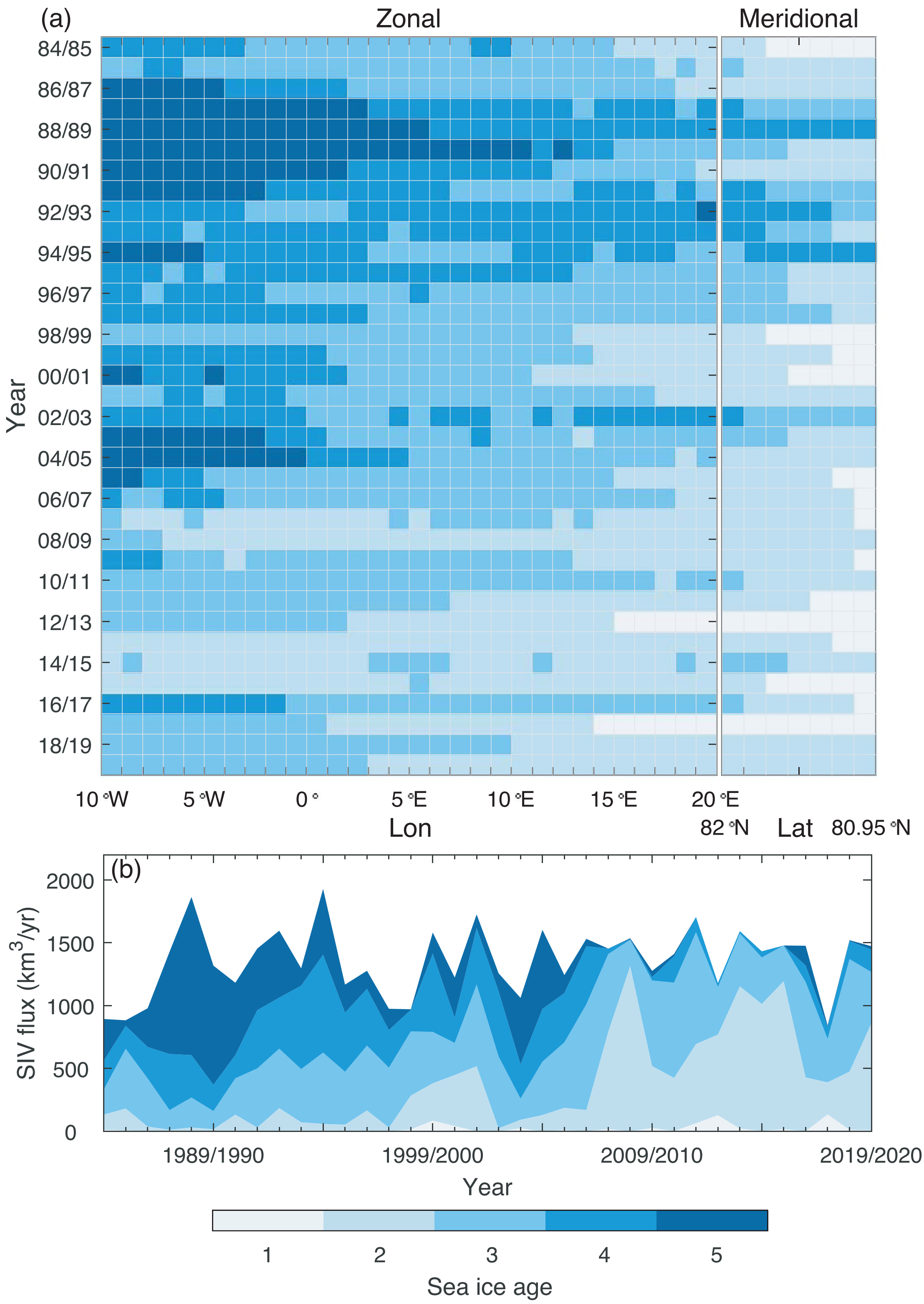

Figure 3. (a) The spatial-temporal variation of the annual mean sea ice age at the Fram Strait from 1984/1985–2019/2020. From top to the bottom is the time variation from 1984/1985–2019/2020. Each horizontal row represents the distribution of the annual mean sea ice age along the Fram Strait for one year. The left part shows the age variation along the zonal gate from 10° W (near Greenland) to 20° E along 82° N, and the right part is for the meridional gate from 82° N to 80.95° N (near Svalbard) along 20° E. (b) Annual total SIV export consists of different ice ages through the Fram Strait from 1984/1985–2019/2020. Note that 2 grids at the west of the zonal gate and 3 grids at the south of the meridional gate lack age values, therefore the sum of volume flux separated by different sea ice ages is slightly lower than the sum of volume flux on the total gate.

the climatology mean of annual SIV flux. The mean annual SIV flux peaks near 5°W on the zonal gate and decreases in both directions along the latitude, which is associated with the East Greenland Current (de Steur *et al* 2009, Spreen *et al* 2020). The only significantly positive trend of annual flux near

Greenland is mainly contributed by variation in SID. The magnitude of fluxes is similar among points of the meridional gate and shows a tiny decrease from 82° N to 80.5° N. Trends on the meridional gate are consistently negative and are statistically significant in higher latitudes. The decreasing trends in fluxes on the meridional gate may link to the shrinking sea ice north of the Svalbard which is induced by the enhanced inflow of the Atlantic water (Shu *et al* 2021).

3.3. Variabilities of the sea ice age and its corresponding fluxes

The evolution of the annual mean sea ice age at the Fram Strait from 1984/1985–2019/2020 is shown in figure 3(a). The annual mean ice age decreases along the zonal gate from Greenland to Svalbard, and older at higher latitudes along the meridional gate. Generally, the annual mean sea ice age at the Fram Strait becomes younger but displays interannual variability. An obvious shift in the sea ice age on the Fram Strait shows around 2007/2008, which could be attributed to the sea ice retreat in 2007 (Maslanik *et al* 2011, Kwok 2018). Before 2008, the zonal gate is covered by a large amount of 3rd-year and 3+ year ice but is mainly 2nd-year ice and 3rd-year ice after 2008. While, an increase in annual mean sea ice age to 4th-year ice shows near Greenland in 2016/2017, which is accounted for a reversal event of Beaufort Gyre in 2016/2017 winter so that the abnormally enhanced SID along the northeast of the Canadian Arctic Archipelago transported more MYI away from the Beaufort Sea to the Fram Strait (Babb *et al* 2020).

Figure 3(b) shows the annual volume flux of different sea ice ages through the Fram Strait from 1984/1985–2019/2020. The annual volume fluxes of different ages show different trends while the trend of total volume flux through the Fram Strait is statistically insignificant. The volume flux of 1st-year significantly increases with the trend of 1.16 km^3 yr^{-2}, but the flux is still a small amount that only occupies 3.5% of the annual SIV flux in the 2010s. While the SIV flux of diverse compositions in MYI varies differently. The volume fluxes of 2nd-year and 3rd-year ice show statistically significant increasing trends of 24.22 km^3 yr^{-2} and 7.99 km^3 yr^{-2}, respectively, and their proportions in the annual SIV flux increased from 6.8% and 25.0% in the 1980s to 49.0% and 38.8% in the 2010s, respectively. However, volume fluxes of 4th-year ice and 5th-year and older (5+ year) ice significantly decreased with the trends of -9.74 km^3 yr^{-2} and -18.28 km^3 yr^{-2}, respectively, and their contribution to the total SIV flux decreased from 22.8% and 45.0% in the 1980s to 7.1% and 1.6% in the 2010s, respectively. Consistent with the evolution of the sea ice age on the Fram Strait, the age composition of annual SIV flux changed dramatically in 2007/2008. Since 2007/2008, almost no 4th-year and 5+ year ice but a large amount of 2nd-year and 3rd-year ice is transported through the Fram Strait, implying a new state of SIV export through the Fram Strait.

4. Conclusions and discussion

SIV export through the Fram Strait is an important dynamic process for regulating sea ice mass and freshwater balance of the Arctic (Lind *et al* 2018, Spreen *et al* 2020, Li *et al* 2022). However, disagreements still surround the magnitude and also trend estimates of the SIV flux across the strait, and analysis is still short of the detailed decomposition of SIV flux according to sea ice age especially the decomposition for MYI. Recent advances in Arctic sea ice data provide a unique opportunity to clarify these issues. NAOSIM can generate more accurate state estimates of Arctic sea ice and preserve the model's conservation by optimizing model parameters with mGA. Additionally, the continuous, complete, and long-term sea ice age record from NSIDC detailed distinguishes sea ice age from 1st-year ice to 5+ year ice. Thus, it is essential to reexamine the above issues by applying the NAOSIM model data and NSIDC sea ice age data.

The mean annual SIV export through the Fram Strait is 1605 ± 315 km^3 yr^{-1} for 1979/1980–2020/2021. Additionally, the insignificant trend of the Fram Strait SIV flux for 1979–2021 by our study confirms the finding in previous studies (e.g. Spreen *et al* 2009, Zhang *et al* 2017, Zamani *et al* 2019). Combining the NSIDC age product with SIV export, we illustrate that although the amount of volume flux changes inconspicuously, the evolution of SIV export at various ages is diverse. As 1st-year ice plays a more important role in the warming Arctic (Kwok 2018), the statistically significant increasing trend of 1st-year ice SIV flux (+1.16 km^3 yr^{-2}) is within our expectation, but it still shows less importance in the total flux with the proportion of 3.5% in the 2010s. For composites in MYI, SIV flux of 2nd-year ice (+24.22 km^3 yr^{-2}) and 3rd-year ice (+7.99 km^3 yr^{-2}) increase significantly, but SIV fluxes of 4th-year ice (-9.74 km^3 yr^{-2}) and 5+ year ice (-18.28 km^3 yr^{-2}) display statistically significant decreasing trends. In addition, the prevailing age of the annual MYI volume export changed obviously since 2007/2008, which could be connected with the extreme SIE retreat and MYI melt in 2007 summer (Maslanik *et al* 2011).

Since our finding reveals an obvious transformation of the predominant age in sea ice outflow via the Fram Strait around 2007/2008 without obvious changes in the amount of volume export, it is necessary to investigate whether the connection between the Fram Strait volume flux and Arctic SIV has changed before and after this time node. The lagged correlation between the monthly anomaly of volume

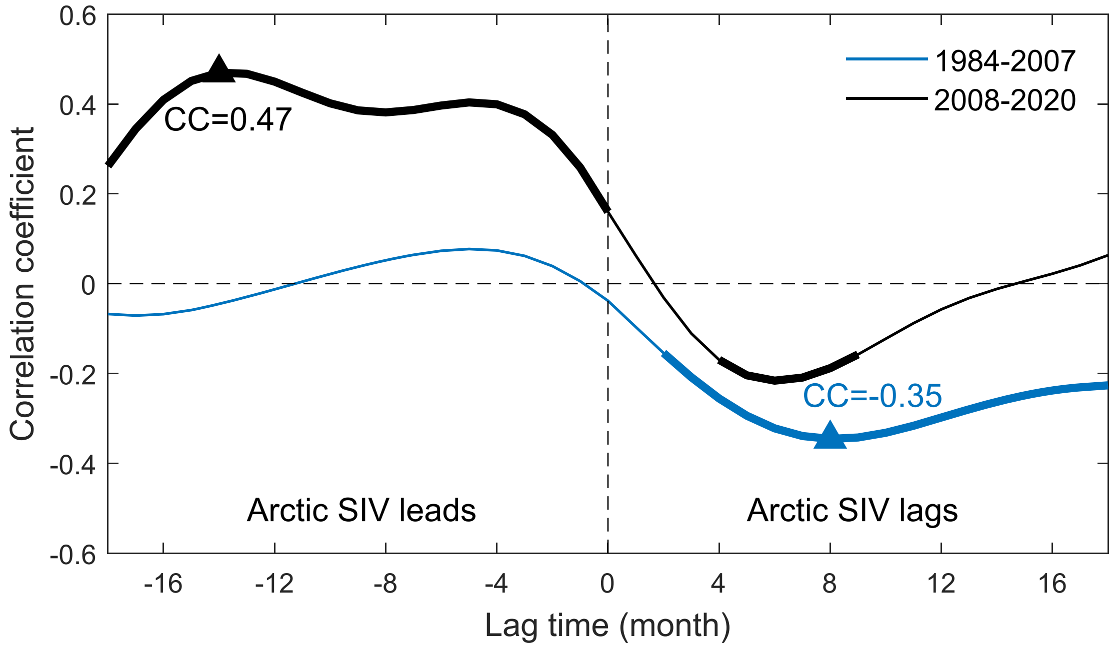

Figure 4. The lagged correlation between the monthly anomaly of the Fram Strait volume flux and the monthly anomaly of Arctic SIV for 1979–2007 (blue line) and 2008–2020 (black line). The Arctic SIV is the sum of the SIV of all grid cells (except for grids southern than the Fram Strait) derived from NAOSIM sea ice thickness and cell area. Positive (negative) lagged time means that Arctic SIV lags (leads) the Fram Strait volume flux, respectively. The time series of volume flux and Arctic SIV are all subjected to a 1-year low-pass Lanczos filter to extract the low-frequency signal. Bold lines represent statistically significant correlation coefficients (CC) at the 95% confidence level, and triangles mark the maximum CC.

flux and the monthly anomaly of Arctic SIV for 1979–2007 and 2008–2020 is examined in figure 4. For 1979–2007, Arctic SIV anomaly is significantly correlated to the Fram Strait volume flux after the lag of 2 months and is most correlated at the lag of 8 months ($CC = -0.35$). The correlation coefficients indicate that the variability of the Fram Strait ice export modulates the variation in Arctic SIV. For 2008–2020, the anomalous Arctic SIV exhibits a significantly positive correlation with the SIV flux anomaly when Arctic SIV leads the SIV flux, which is not shown before 2008, and it is most correlated when the Arctic SIV leads the SIV flux by 14 months ($CC = 0.47$). The result illustrates that the variability of volume export becomes the response of variation in Arctic SIV when sea ice outflow becomes younger. Meanwhile, the negative correlation when Arctic SIV lags the volume flux decreases compared with 1979–2007. Thus, the preceding effect of the anomalous Fram Strait SIV export on Arctic SIV variability declines with the change of sea ice age in SIV export, which implies that local thermodynamic and dynamic processes in the Arctic rather than sea ice export might be responsible for the anomaly of Arctic SIV in recent years (Wei *et al* 2019).

The Fram Strait and northern Svalbard are key regions for oceanic heat supply to the Arctic Ocean by the warm Atlantic Water and are the place of ocean-sea ice interaction (Wang *et al* 2020). Under the situation of younger sea ice outflow and inconspicuous change in the amount of SIV flux, the larger mass of freshwater flux brought by sea ice can be transported to the Atlantic through the Fram Strait considering the larger density of younger sea ice than older sea ice (Zygmuntowska *et al* 2014), which may further influence the dense water formation in the North Atlantic Ocean (Ionita *et al* 2016, Sumata *et al* 2022). However, further comprehensive investigations are still needed on this subject.

Meanwhile, uncertainties still exist within NAOSIM model data and NSIDC sea ice age product which may cause bias in our estimation. Compared with ULS-thickness based estimates near 79° N (Vinje *et al* 1998, Kwok and Rothrock 1999, Kwok *et al* 2004, Spreen *et al* 2020), the NAOSIM derived SIV flux at 79° N (figure not shown) is basically within the uncertainties of estimations obtained by *in-situ* observation of SIT although NAOSIM underestimates SIV flux in the freezing season. It is also worth noting that the spatial scarcity of *in-situ* observations may cause uncertainties in SIV flux estimation. Meanwhile, large discrepancies in SIV flux estimations can be induced by using different sources of SID data, even if the same SIT data is adopted (Vinje *et al* 1998, Kwok and Rothrock 1999, Spreen *et al* 2020). Moreover, results combining the sea ice age data in this study may overestimate the sea ice age, which is induced through the derivation of NSIDC age product (Tschudi *et al* 2020). In the future, we plan to further examine the causes and impacts of the reversal relation between sea ice export via the Fram Strait and Arctic SIV under the dramatically changing Arctic. The effect of the Fram Strait SIV outflow on ocean processes is also considered in our future investigations.

Data availability statement

The sea ice age product (10.5067/UTAV7490FEPB) and sea ice motion vectors (10.5067/INAWUWO7QH7B) are accessible from the National Snow and Ice Data Center. The CS2SMOS data is available from ftp://ftp.awi.de/sea_ice/product/cryosat2/v2p4/.

All data that support the findings of this study are included within the article (and any supplementary files).

Acknowledgments

This study was funded by the National Natural Science Foundation of China (No. 41922044, 41941009, 42006191), the National Key R&D Program of China (No. 2022YFE0106300), the Guangdong Basic and Applied Basic Research Foundation (No. 2020B1515020025), the fundamental research funds for the Norges Forskningsråd (No. 328886), and the Innovation Group Project of Southern Marine Science and Engineering Guangdong Laboratory (Zhuhai) (311021008). We thank NSIDC for providing the sea ice age and sea ice motion data. The production of the merged CryoSat-SMOS sea ice thickness data was funded by the ESA project SMOS & CryoSat-2 Sea Ice Data Product Processing and Dissemination Service, and data from DATE to DATE were obtained from AWI.

Conflict of interest

The authors declare no conflicts of interest.

ORCID iDs

Chao Min https://orcid.org/0000-0002-4181-2107
Hao Luo https://orcid.org/0000-0002-3707-3794
Robert Ricker https://orcid.org/0000-0001-6928-7757

References

Arfeuille G, Mysak L A and Tremblay L B 2000 Simulation of the interannual variability of the wind-driven Arctic sea-ice cover during 1958–1998 *Clim. Dyn.* **16** 107–21

Babb D G, Landy J C, Lukovich J V, Haas C, Hendricks S, Barber D G and Galley R J 2020 The 2017 reversal of the Beaufort Gyre: can dynamic thickening of a seasonal ice cover during a reversal limit summer ice melt in the Beaufort Sea? *J. Geophys. Res.* **125** e2020JC016796

Balmaseda M A *et al* 2015 The ocean reanalyses intercomparison project (ORA-IP) *J. Oper. Oceanogr.* **8** s80–s97

Bi H, Fu M, Sun K, Liu Y, Xu X and Huang H 2016 Arctic sea ice thickness changes in terms of sea ice age *Acta Oceanol. Sin.* **35** 1–10

Bi H, Wang Y, Zhang W, Zhang Z, Liang Y, Zhang Y, Hu W, Fu M and Huang H 2018b Recent satellite-derived sea ice volume flux through the Fram Strait: 2011–2015 *Acta Oceanol. Sin.* **37** 107–15

Bi H, Zhang J, Wang Y, Zhang Z, Zhang Y, Fu M, Huang H and Xu X 2018a Arctic sea ice volume changes in terms of age as revealed from satellite observations *IEEE J. Sel. Top. Appl. Earth Obs. Remote Sens.* **11** 2223–37

de Steur L, Hansen E, Gerdes R, Karcher M, Fahrbach E and Holfort J 2009 Freshwater fluxes in the East Greenland current: a decade of observations *Geophys. Res. Lett.* **36** L23611

Gerdes R, Karcher M J, Kauker F and Schauer U 2003 Causes and development of repeated Arctic Ocean warming events *Geophys. Res. Lett.* **30** 1980

Haine T *et al* 2015 Arctic freshwater export: status, mechanisms, and prospects *Glob. Planet Change* **125** 13–35

Ionita M, Scholz P, Lohmann G, Dima M and Prange M 2016 Linkages between atmospheric blocking, sea ice export through Fram Strait and the Atlantic Meridional overturning circulation *Sci. Rep.* **6** 32881

Karcher M, Beszczynska-Möller A, Kauker F, Gerdes R, Heyen S, Rudels B and Schauer U 2011 Arctic Ocean warming and its consequences for the Denmark Strait overflow *J. Geophys. Res.* **116** C02037

Karcher M, Kauker F, Gerdes R, Hunke E and Zhang J 2007 On the dynamics of Atlantic Water circulation in the Arctic Ocean *J. Geophys. Res.* **112** C04S02

Kauker F, Gerdes R, Karcher M and Köberle C 2005 Impact of North Atlantic Current changes on the Nordic Seas and the Arctic Ocean *J. Geophys. Res.* **110** C12002

Krumpen T, Gerdes R, Haas C, Hendricks S, Herber A, Selyuzhenok V, Smedsrud L and Spreen G 2016 Recent summer sea ice thickness surveys in Fram Strait and associated ice volume fluxes *Cryosphere* **10** 523–34

Kwok R 2018 Arctic sea ice thickness, volume, and multiyear ice coverage: losses and coupled variability (1958–2018) *Environ. Res. Lett.* **13** 105005

Kwok R, Cunningham G F and Pang S S 2004 Fram Strait sea ice outflow *J. Geophys. Res.* **109** C01009

Kwok R and Rothrock D A 1999 Variability of Fram Strait ice flux and North Atlantic oscillation *J. Geophys. Res.* **104** 5177–89

Kwok R and Rothrock D A 2009 Decline in Arctic sea ice thickness from submarine and ICESat records: 1958-2008 *Geophys. Res. Lett.* **36** L15501

Li X, Yang Q, Yu L, Holland P R, Min C, Mu L and Chen D 2022 Unprecedented Arctic sea ice thickness loss and multiyear-ice volume export through Fram Strait during 2010–2011 *Environ. Res. Lett.* **17** 095008

Lind S, Ingvaldsen R B and Furevik T 2018 Arctic warming hotspot in the northern Barents Sea linked to declining sea-ice import *Nat. Clim. Change* **8** 634–9

Maslanik J A, Fowler C, Stroeve J, Drobot S, Zwally J, Yi D and Emery W 2007 A younger, thinner Arctic ice cover: increased potential for rapid, extensive sea-ice loss *Geophys. Res. Lett.* **34** L24501

Maslanik J, Stroeve J, Fowler C and Emery W 2011 Distribution and trends in Arctic sea ice age through spring 2011 *Geophys. Res. Lett.* **38** L13502

Meredith M *et al* 2019 *Polar Regions In: IPCC Special Report on the Ocean and Cryosphere in a Changing Climate* (Cambridge: Cambridge University Press) pp 203–320

Min C, Mu L, Yang Q, Ricker R, Shi Q, Han B, Wu R and Liu J 2019 Sea ice export through the Fram Strait derived from a combined model and satellite data set *Cryosphere* **13** 3209–24

Ricker R, Girard-Ardhuin F, Krumpen T and Lique C 2018 Satellite-derived sea ice export and its impact on Arctic ice mass balance *Cryosphere* **12** 3017–32

Ricker R, Hendricks S, Kaleschke L, Tian-Kunze X, King J and Haas C 2017 A weekly Arctic sea-ice thickness data record from merged CryoSat-2 and SMOS satellite data *Cryosphere* **11** 1607–23

Ricker R, Kauker F, Schweiger A, Hendricks S, Zhang J and Paul S 2021 Evidence for an increasing role of ocean heat in Arctic winter sea ice growth *J. Clim.* **34** 5215–27

Saha S *et al* 2014 The NCEP climate forecast system version 2 *J. Clim.* **27** 2185–208

Selyuzhenok V, Bashmachnikov I, Ricker R, Vesman A and Bobylev L 2020 Sea ice volume variability and water temperature in the Greenland Sea *Cryosphere* **14** 477–95

Serreze M C, Barrett A P, Slater A G, Woodgate R A, Aagaard K, Lammers R B, Steele M, Moritz R, Meredith M and Lee C M 2006 The large-scale freshwater cycle of the Arctic *J. Geophys. Res.* **111** C11010

Shu Q, Wang Q, Song Z and Qiao F 2021 The poleward enhanced Arctic Ocean cooling machine in a warming climate *Nat. Commun.* **12** 2966

Spreen G, Kern S, Stammer D and Hansen E 2009 Fram Strait sea ice volume export estimated between 2003 and 2008 from satellite data *Geophys. Res. Lett.* **36** L19502

Spreen G, Steur L, Divine D, Gerland S, Hansen E and Kwok R 2020 Arctic sea ice volume export through Fram Strait from 1992 to 2014 *J. Geophys. Res.* **125** e2019JC016039

Sumata H, de Steur L, Gerland S, Divine D V and Pavlova O 2022 Unprecedented decline of Arctic sea ice outflow in 2018 *Nat. Commun.* **13** 1747

Sumata H, Kauker F, Karcher M and Gerdes R 2019a Simultaneous parameter optimization of an Arctic sea ice–ocean model by a genetic algorithm *Mon. Weather Rev.* **147** 1899–926

Sumata H, Kauker F, Karcher M and Gerdes R 2019b Covariance of optimal parameters of an Arctic Sea ice–ocean model *Mon. Weather Rev.* **147** 2579–602

Tschudi M A, Meier W N and Stewart J S 2020 An enhancement to sea ice motion and age products at the National Snow and Ice Data Center (NSIDC) *Cryosphere* **14** 1519–36

Tschudi M A, Stroeve J C and Stewart J S 2016 Relating the age of Arctic Sea ice to its thickness, as measured during NASA's ICESat and IceBridge campaigns *Remote Sens.* **8** 457

Tschudi M, Meier W N, Stewart J S, Fowler C and Maslanik J 2019a *Polar Pathfinder Daily 25 km EASE-Grid Sea Ice Motion Vectors, Version 4* (Boulder, CO: NASA National Snow and Ice Data Center Distributed Active Archive Center) (https://doi.org/10.5067/INAWUWO7QH7B)

Tschudi M, Meier W N, Stewart J S, Fowler C and Maslanik J 2019b *EASE-Grid Sea Ice Age, Version 4* (Boulder, CO: NASA National Snow and Ice Data Center Distributed Active Archive Center) (https://doi.org/10.5067/UTAV7490FEPB)

Vinje T, Nordlund N and Kvambekk Å 1998 Monitoring ice thickness in Fram Strait *J. Geophys. Res.* **103** 10437–49

Wang Q, Wekerle C, Wang X, Danilov S, Koldunov N, Sein D, Sidorenko D, von Appen W J and Jung T 2020 Intensification of the Atlantic water supply to the arctic ocean through Fram Strait induced by Arctic sea ice decline *Geophys. Res. Lett.* **47** e2019GL086682

Wang Y, Bi H and Liang Y 2022 A satellite-observed substantial decrease in multiyear ice area export through the Fram Strait over the last decade *Remote Sens.* **14** 2562

Wei J, Zhang X and Wang Z 2019 Reexamination of Fram Strait sea ice export and its role in recently accelerated Arctic sea ice retreat *Clim. Dyn.* **53** 1823–41

Zamani B, Krumpen T, Smedsrud L H and Gerdes R 2019 Fram Strait sea ice export affected by thinning: comparing high-resolution simulations and observations *Clim. Dyn.* **53** 3257–70

Zhang Z, Bi H, Sun K, Huang H, Liu Y and Yan L 2017 Arctic sea ice volume export through the Fram Strait from combined satellite and model data: 1979–2012 *Acta Oceanol. Sin.* **36** 44–55

Zygmuntowska M, Rampal P, Ivanova N and Smedsrud L H 2014 Uncertainties in Arctic sea ice thickness and volume: new estimates and implications for trends *Cryosphere* **8** 705–20